European Polymer Journal 164 (2022) 110975

Contents lists available at ScienceDirect

European Polymer Journal

journal homepage: www.elsevier.com/locate/europolj

Synthesis of colorless polyimides with high T_g from asymmetric twisted benzimidazole diamines

Xiaoying Yan, Fengna Dai, Zhao Ke, Kuangguo Yan, Chunhai Chen, Guangtao Qian *, Hui Li *

[a] Center for Advanced Low-Dimension Materials, State Key Laboratory for Modification of Chemical Fibers and Polymer Materials, College of Material Science and Engineering, Donghua University, Shanghai 201620, P. R. China

ARTICLE INFO

Keywords:
Colorless polyimides
High T_g
Poly(benzimidazole imide)s
Twisted structures

ABSTRACT

To prepare colorless polyimide (CPI) films with high thermal properties, an effective design strategy is incorporating asymmetric and twisted structures in the polymer chain-segments. Based on this strategy, 6,4′-diamino-2′-methyl-1-methyl-2-phenylbenzimidazole (5a) and 6,4′-diamino-2′-trifluoromethyl-1-methyl-2-phenylbenzimidazole (5b) were synthesized, and two series of their polyimides (semi- and fully aromatic series) were prepared, respectively. The obtained poly(benzimidazole imide)s (PBIIs) with loosely packed but rigid backbones possessed not only high glass transition temperature (T_g) but also improved optical transparency. In particular, the semi-aromatic system achieved an excellent transmittance about 80% at 400 nm and an outstanding T_g exceeding 400 °C. Furthermore, the influence of various 2′-substitutions on the combination properties of these poly(benzimidazole imide)s was systematically analyzed. These data expand the poly(benzimidazole imide)s as optical materials and provide a feasible method to prepare heat-resistant colorless polymers.

1. Introduction

Colorless polymers with their remarkable lightweight and flexibility, as potential alternatives to fragile inorganic glass, are the most popular candidates for reliable substrates in next-generation image displays [1–3]. These optimal plastic materials must possess both outstanding optical transparency and super heat resistance to meet the functional and manufacturing requirements of optical components [4,5]. For example, in the primary fabrication of various display devices, the solder-reflowing temperature is up to 260 °C, and the processing temperature of thin-film transistor exceeds 400 °C (short term) [4,6]. Hence, the glass transition temperature of the selected polymers is supposed to at least 300 °C, more desirably > 400 °C. Most optical polymer films, such as polyethylene terephthalate (T_g = 78 °C), polyethylene naphthalate (T_g = 120 °C) and polycarbonate (T_g = 150 °C), cannot overcome the high processing temperature; even poly (ether sulfone) (T_g = 220 °C), as one of the current colorless engineering polymers with the highest heat resistance, is insufficient for the harsh fabrication processes [7–10]. Thus, colorless polymers with high-temperature resistance are required urgently in industry and science.

Polyimides with super heat-resistance grade are widely used in aeronautical, microelectronic and electric devices [11–13]. Their T_gs can reach >300 °C, e. g., Novax (T_g = 350 °C), Kapton H (T_g = 385 °C) and Upilex S (T_g > 500 °C) [14]. The extraordinary thermal properties are attributed to their conjugated rigid backbones and dense backbone packing. However, the intensive coloration of these polymer films disturbs their optical applications. Much current research has been done to achieve colorless polyimides [15–18]. According to the charge transfer complex (CTC) formation theory [19,20], the efficient approaches are to disturb chain conjugations, reduce packing coefficient and optimize monomer activity (electron-donating ability of diamines, electron-withdrawing ability of dianhydrides) [21]. Among these, rational structural manipulations include employment of geometrically asymmetric structures, bulky substituents, noncoplanar moieties or flexible ether, use of alicyclic dianhydrides, and introduction of trifluoromethyl (–CF_3). Specifically, incorporating bulky substituents or flexible linkage can prevent effective chain packing, and lead to weakened charge transfer (CT) interaction, whereas the method provides colorless polyimides with insufficiently high thermal properties because of their excessively reduced intermolecular interactions [22,23]. Fortunately, use of asymmetric or noncoplanar groups can perfectly overcome the problem. The asymmetric units with significant steric hindrance can forbid the chain-segment π-flip rotational motions to bring favorable T_gs of the corresponding polyimides [24–26]; also, the rigid but non-

* Corresponding author.
E-mail addresses: qgt@dhu.edu.cn (G. Qian), lihui@dhu.edu.cn (H. Li).

https://doi.org/10.1016/j.eurpolymj.2021.110975
Received 26 October 2021; Received in revised form 1 December 2021; Accepted 23 December 2021
Available online 29 December 2021

coplanar monomers possess the identical effect, and, 2,2′-bis(trifluoromethyl)benzidine (TFMB) and 2,2′-dimethylbenzidine (DMBZ) are representative cases [27,28].

Among many diamine monomers for polyimides, 5(6)-amino-2-(4-aminobenzene)benzimidazole (PABZ) has a rigid and asymmetric skeleton structure. The polyimides made from PABZ exhibit T_gs > 400 °C, which leads to their research as thermal-resistant fabrications [29–31], however, no attention has been paid to develop them as optical films. The primary cause is that poly(benzimidazole imide) films show dark coloration, mainly due to their high packing coefficient and strong intermolecular interaction derived from the particular hydrogen bonds [32,33]. In our previous discussion, N-substituent can be used as an effective incorporation to hinder hydrogen-bonds formation and loosen chain packing, which provides an effective way to enhance the optical transparency of poly(benzimidazole imide)s without losing their superior thermal properties [33]. Based on the strategy, 2′-substituted N-methyl (N-CH_3) benzimidazole diamines are expected to gather the superiority of PABZ and TFMB (or DMBZ) (Fig. 1), that is, the asymmetric, noncoplanar and rigid monomers may provide polyimides with enhanced optical and thermal properties.

In the present study, two novel benzimidazole diamines containing N-CH_3 and 2′- substituents were synthesized according to Scheme 1. The modified PBIIs were prepared through a one-stage procedure (Scheme 2) with the obtained diamines, including semi- and fully- aromatic series. The influence of different polymer configuration on their chain packing and properties were systematically investigated and analyzed. These data provide a feasible framework to expand poly(benzimidazole imide) s application as heat-resistant colorless polymers.

2. Experimental

2.1. Materials

2-methyl-4-nitrobenzoic acid, 4-nitro-2-(trifluoromethyl)benzoic acid, N-methyl-4-nitrobenzene-1,2-diamine and sulfinyl chloride ($SOCl_2$) were purchased from Shanghai Aladdin Biochemical Technology Co., Ltd. 4,4-(hexafluoroisopropylidene) diphthalic anhydride (6FDA) and *p*-toluenesulfonic acid (*p*-TSA) were obtained from Tokyo Chemical Industry (Shanghai). 1,2,4,5-cyclohexanetetracarboxylic dianhydride (HPMDA) was supplied by Sinopharm Chemical Reagent Shanghai Co., Ltd. Triethylamine (Et_3N), palladium 10% on charcoal (Pd/C), 98% hydrazine monohydrate ($N_2H_4{\cdot}H_2O$) and other solvents (analytical-reagent grade) were purchased from Sinopharm Chemical Reagent Shanghai Co., Ltd and used as received. All the commercially available dianhydrides were dried at 150 °C in a vacuum oven for 24 h to eliminate the effect of water before use.

2.2. Characterization

Nuclear magnetic resonance (NMR) spectra were obtained on a 600 MHz Avance III spectrometer (Bruker, Billerica, MA), in which dimethyl sulfoxide-d_6 was used as a solvent. Elemental analysis was carried out by a Vario EL-III elemental analyzer (Elmentar, Hanau, Germany). The melting point was measured using digital melting point apparatus WRS-2C (INESA Physico-Optical Instrument, Shanghai,China) at a heating rate of 2 °C min^{-1}. Attenuated total reflectance fourier transform infrared (ATR-FTIR) spectra were conducted on a Nicolet 6700 infrared spectrometer (ThermoFisher, Waltham, MA) by averaging 32 scans within the range of 4000-400 cm^{-1}. The number-average (M_n) and weight-average (M_w) molecular weights were measured by gel permeation chromatography (Waters GPC Systems, Milford, MA) with polystyrene as an external standard and NMP as the eluent. The transmittance of the films was recorded on a UV-3600 spectrophotometer (Shimadzu, Kyoto, Japan) with the wavelength range of 200–800 nm. Color intensities were assessed by a CS-720 colorimeter (Hangzhou color spectrum Co. LTD., China) with an observational angle of 10°. Wide angle X-ray diffraction (WAXD) spectra were collected on a Rigaku Denki D/MAX-2500 diffractometer (Rigaku, Tokyo, Japan) with Cu Kα radiation ($\lambda = 1.54$ Å) at room temperature. Thermogravimetric analysis (TGA), Dynamic mechanical analysis (DMA) and Coefficient of thermal expansion (CTE) were assessed using Discovery TGA 550, DMA Q800 and TMA Q400 (TA Instrument, New Castle, DE), with a constant heating rate of 5 °C min^{-1} under nitrogen, respectively. Mechanical properties of polymer films were evaluated on an Instron 5966 universal testing machine (Instron, Boston, MA) at speed of 5 mm min^{-1}, and tensile modulus (E), tensile strength (σ), and elongation at break (ε) were demonstrated as the average of five strips. The solubility of polymers was qualitatively determined using 10 mg of a sample in 1 mL of the solvent.

The net charges and geometry-optimized structures of the diamines (5a and 5b) were achieved through the GGA-BLYP/DND method for Dmol3 module in Materials Studio 2019 program (Accelrys, San Diego, CA) [34,35]. The conformation rotation of the single bond between imidazole ring and benzene ring was conducted using the conformer tools in Material Studio and the geometry of the repeat unit was optimized by COMPASS force-field [36,37].

Densities of the films were collected using a XS204 densimeter (Mettler Toledo, Zurich, Swiss) by the buoyancy method with anhydrous ethanol (Sigma-Aldrich) as a medium. The fractional free volume (FFV) was calculated from Eq. (1):

$$FFV = \frac{V - V_0}{V} \tag{1}$$

$$V = \frac{M_0}{\rho} \tag{2}$$

$$V_0 = 1.3 \cdot V_w \tag{3}$$

where V is the actual molar volume including the free volume and the occupied molar volume (V_0), which is determined by the molecular mass (M_0) of the repeating unit and the measured density (ρ) of the films (Eq. (2)). Empirically, the V_0 is 1.3 times as large as its V_W (Eq. (3)) [38]. V_W is the van der Waals molar volume, and the value is calculated from a group contribution theory using the Synthia module from Materials Studio [18,39].

Water absorption (W_A) of the films was confirmed by the weight differences before and after placing in distilled water. Typically, the film samples with dimensions of 50 × 50 mm were dried in a vacuum oven and weighed. After being placed in water bath at 25 °C for 24 h, the specimens were wiped clean and weighed. The water absorption is were determined by Eq. (4)

$$W_A = \frac{m_2 - m_1}{m_1} \times 100\% \tag{4}$$

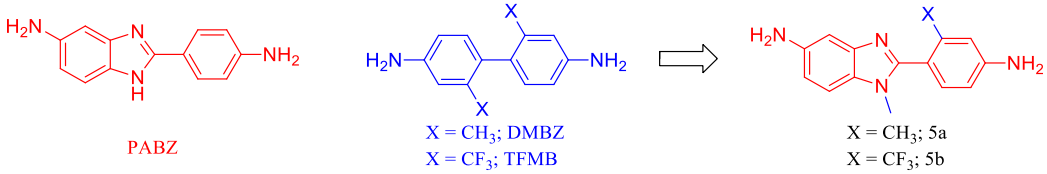

Fig. 1. Novel benzimidazole diamines derived from some commercial diamine structures.

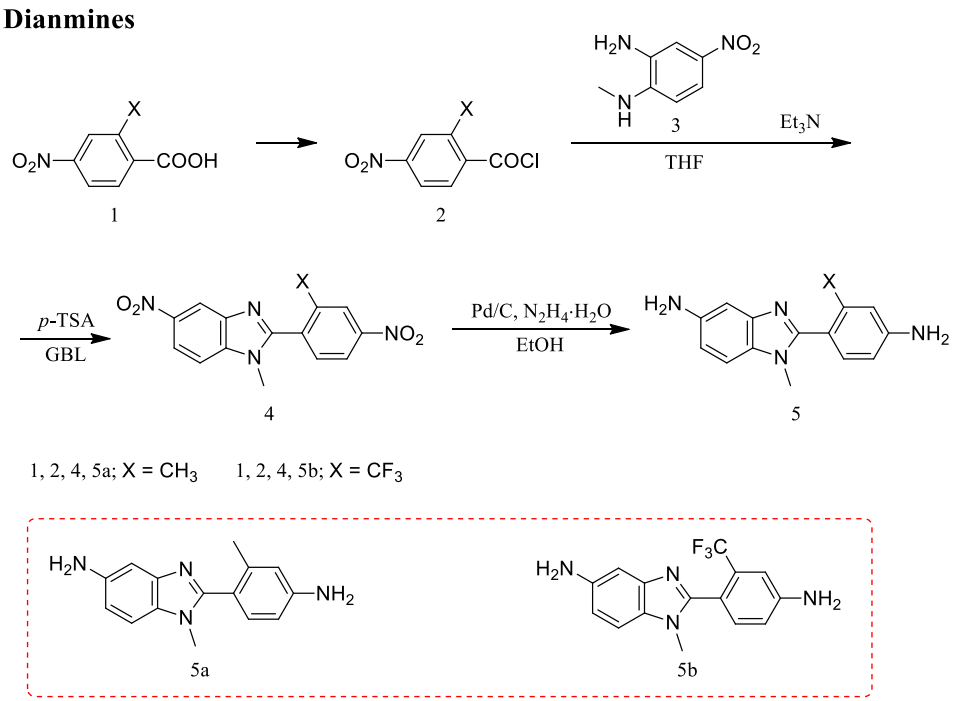

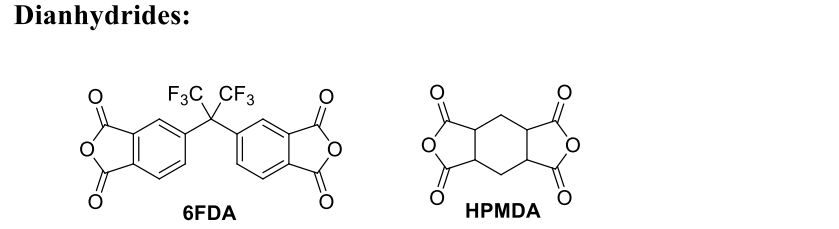

Scheme 1. Synthesis of the benzimidazole diamines and chemical structures of dianhydrides used for polymerization.

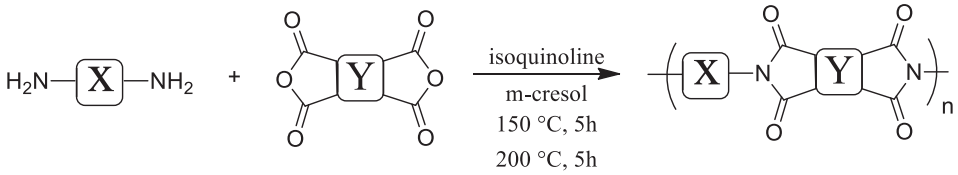

Scheme 2. Synthetic routes of the poly(benzimidazole imide)s.

where m_1 and m_2 are the sample's dry mass and its wet mass after being soaked, respectively. W_A is the mean value of three parallel samples.

2.3. Synthesis of diamines

2.3.1. 6,4′-dinitro-2′-methyl-1-methyl-2-phenylbenzimidazole (4a)

In ice-water bath, N-methyl-4-nitrobenzene-1,2-diamine (5.34 g, 32.0 mmol), Et_3N (3.88 g, 38.4 mmol) and THF (40 mL) were poured into a 100 mL flask equipped with magnetic stirrer, then 2-methyl-4-nitrobenzoyl chloride (7.64 g, 38.4 mmol, experimental data was supplied in the supporting information) was added dropwise over 30 min. After stirring for 12 h, the mixture was precipitated into methanol. The precipitate was filtered, washed with methanol and dried under vacuum to obtain yellow crude product (8.87 g). Then, the obtained powder and *p*-TSA (5.10 g, 29.6 mmol) were dissolved in 1,4-butyrolactone (GBL, 80 mL) and heated to 200 °C to achieve cyclization, and the reaction solution was precipitated in water to give an off-white crude product. The crude product was recrystallized in DMSO to give a golden yellow solid 4a (7.6 g, two-step yield: 76.1%). Melting point: 279 °C. ^{1}H NMR (DMSO-d_6, ppm): δ = 8.63 (d, J = 2.1 Hz, 1H), 8.36 (d, J = 2.4 Hz, 1H), 8.28 (dd, J = 9.0, 2.2 Hz, 1H), 8.25–8.20 (m, 1H), 7.92 (d, J = 9.0 Hz, 1H), 7.85 (d, J = 8.4 Hz, 1H), 3.74 (s, 3H), 2.38 (s, 3H). FTIR (KBr, ν, cm^{-1}): 1524, 1355 (NO_2 asymmetric and symmetric stretching); 1611, 1465 (C═N/C═C stretching of ring). Anal. Calcd for $C_{15}H_{12}N_4O_4$: C, 57.69%; H, 3.87%; N, 17.94%. Found: C, 57.37%; H, 3.94%; N, 18.33%.

2.3.2. 6,4′-diamino-2′-methyl-1-methyl-2-phenylbenzimidazole (5a)

A mixture of 4a (5.0 g, 16.01 mmol), Pd/C (0.5 g) and absolute ethanol (50 mL) were added into a 100 mL flask fitted with reflux condenser and heated to 80 °C. The $N_2H_4{\cdot}H_2O$ (8.0 mL) was added dropwise over a period of 30 min, and then the reaction mixture was refluxed at 80 °C for 3 h. The progress of the reaction was monitored by thin layer chromatography (TLC). After the completion of the reaction, the catalyst of Pd/C was removed by hot filtration, and deionized water was poured into the reaction solution to precipitate white product. It was filtered, washed with water and dried at 80 °C in vacuum oven for

24 h to yield white power (3.5 g, yield: 87.3%). Melting point: 102 °C. ^{1}H NMR (DMSO-d_6, ppm): δ = 7.16 (d, J = 8.4 Hz, 1H), 7.00 (d, J = 8.1 Hz, 1H), 6.79–6.74 (m, 1H), 6.59 (dd, J = 8.5, 2.1 Hz, 1H), 6.55–6.45 (m, 2H), 5.32 (s, 2H), 4.68 (s, 2H), 3.47 (s, 3H), 2.07 (s, 3H).^{13}C NMR (DMSO-d_6, ppm): δ = 153.73, 150.02, 144.36, 144.28, 138.51, 131.45, 128.81, 117.76, 115.56, 111.73, 111.44, 110.28, 102.71, 30.90, 20.23. FTIR (KBr, ν, cm^{-1}): 3436, 3324, 3208 (amine NH); 1615, 1491 (C═N/C═C stretching of ring), 1319 (imidazole ring breathing). Anal. Calcd for $C_{15}H_{16}N_4$: C, 71.40%; H, 6.39%; N, 22.21%. Found: C, 71.25%; H, 6.65%; N, 22.07%.

5b was synthesized by a similar method of 5a but with 4-nitro-2-(trifluoromethyl)benzoic acid (experimental data was supplied in the supporting information) as a starting material.

2.3.3. 6,4′-dinitro-2′-trifluoromethyl-1-methyl-2-phenylbenzimidazole (4b)

A light yellow powder (two-step yield: 74.2%). Melting point: 254 °C. ^{1}H NMR (DMSO-d_6, ppm): δ = 8.76–8.68 (m, 2H), 8.65 (d, J = 2.1 Hz, 1H), 8.30 (dd, J = 9.0, 2.2 Hz, 1H), 8.19 (d, J = 8.3 Hz, 1H), 7.95 (d, J = 9.0 Hz, 1H), 3.72 (s, 3H). FTIR (KBr, ν, cm^{-1}): 1521, 1342 (NO_2 asymmetric and symmetric stretching); 1614, 1469 (C═N/C═C stretching of ring). Anal. Calcd for $C_{15}H_9F_3N_4O_4$: C, 49.19%; H, 2.48%; N, 15.30%. Found: C, 49.02%; H, 2.60%; N, 15.69%.

2.3.4. 6,4′-diamino-2′-trifluoromethyl-1-methyl-2-phenylbenzimidazole (5b)

A white powder (yield: 90%). Melting point: 140 °C. ^{1}H NMR (DMSO-d_6, ppm): δ = 7.19 (d, J = 8.3 Hz, 2H), 7.03 (d, J = 2.3 Hz, 1H), 6.87 (dd, J = 8.3, 2.3 Hz, 1H), 6.77 (d, J = 2.0 Hz, 1H), 6.62 (dd, J = 8.5, 2.1 Hz, 1H), 5.93 (s, 2H), 4.73 (s, 2H), 3.41 (s, 3H). ^{13}C NMR (DMSO-d_6, ppm): δ = 150.99, 150.63, 144.52, 144.12, 133.43, 129.80 (q, J = 29.5 Hz), 128.64, 124.37 (q, J = 273.9 Hz), 116.44, 115.23 (q, J = 2.2 Hz), 112.28, 110.99 (q, J = 5.0 Hz), 110.40, 102.80, 30.70. FTIR (KBr, ν, cm^{-1}): 3448, 3343, 3227 (amine NH); 1626, 1480 (C═N/C═C stretching of ring). Anal. Calcd for $C_{15}H_{13}F_3N_4$: C, 58.82%; H, 4.28%; N, 18.29%. Found: C, 58.58%; H, 4.46%; N, 17.98%.

2.4. Synthesis of polymers

The poly(benzimidazole imide)s were prepared by using a conventional one-stage procedure in *m*-cresol with isoquinoline, as shown as Scheme 2. Using the process of 5a-6FDA as a representative example, 6FDA (0.8885 g, 2.0 mmol) was added in a solution of 5a (0.5046 g, 2.0 mmol) in *m*-cresol (5.6 g) at room temperature under nitrogen atmosphere. After being stirred at 150 °C for 5 h, to the mixture was added isoquinoline (0.0258 g, 0.2 mmol). The reaction solution was held at 200 °C for additional 5 h. Then, it was cooled, poured into 100 mL ethanol and stirred overnight. The fibrous polyimide was collected by filtration and washing with ethanol. The desired product was dried at 100 °C under vacuum for 24 h to give 5a-6FDA. The PI powder was redissolved in DMAc at a solid content of 15 wt%. Then, the PI solution was cast on a glass plate and dried at 200 °C for 2 h under vacuum. The PI film (typically 20 μm thick) could be got after being peeled off from the substrate with boiling deionized water.

3. Results and discussion

3.1. Molecular structure and characterization

2′–CH_3 and 2′-CF_3 substituted N-methyl benzimidazole diamines were successfully synthesized through the reaction sequence depicted in Scheme 1. In the FTIR spectrum of the synthesized diamine monomers (Fig. S1), the characteristic absorptions of —NH_2 stretching bands (3385–3202 cm^{-1}) could be clearly observed, but the absorption bands (near 1355 and 1524 cm^{-1}) corresponding to —NO_2 symmetric and asymmetric stretching disappeared, confirming the obtained —NH_2 terminals. The ^{1}H NMR spectrum (Fig. 2) further proved the results. Specifically, two obvious amine proton signals appeared in the spectra of both 5a and 5b, indicative of their asymmetric structures. The signals at around 4.85 ppm attributed to the amine protons linked to benzimidazole ring, and the signals at about 5.25 ppm (5a) and 5.85 ppm (5b) could be assigned to the amine protons attached to the phenyl ring. In the result, the 2′-substituent nature significantly affected the chemical shifts of the amine protons on the substituted aniline, that is, the —NH_2 group in the 2′-CF_3 based diamine would possess inferior nucleophilicity than the 2′-CH_3-one owing to the electron withdrawing effect of the trifluoromethyl moiety. Furthermore, to better confirm the structure of these monomers, the ^{1}H NMR spectrum (Fig. S2) and ^{13}C NMR spectrum (Fig. S3) had been given and the data was accorded with the expected structure. To understand the monomers more, the net charges and geometries were calculated by the Dmol3 program based on the Materials Studio software (Fig. 3). Obviously, the N atom of amines on the 2′-CF_3 substituted aniline showed lower net charges than the one on the 2′-CH_3 substituted aniline, which agreed with the nucleophilicity order from the results of ^{1}H NMR. The phenomenon further suggested that the introduction of the strong electron-withdrawing trifluoromethyl would reduce the electron-donating effect of the corresponding diamine.

3.2. Polymerization and molecular packing

The semi- and fully- aromatic PBIIs were prepared via a traditional one-step method in m-cresol, using isoquinoline as the catalyst, as shown in Scheme 2. The PBII number-average molecular weights were in the range of 4.26–5.70 × 10^4 g mol^{-1} (Table 1), reflecting their sufficient molecular weights. The M_ns were believed to be susceptible to the reactivity of monomers, that is, the higher reactivity would induce higher polycondensation degree, resulting in higher M_n values [35]. In this work, the poly(benzimidazole imide)s derived from 5a had a higher M_ns than those with 5b, for a given dianhydride, which was exactly in agreement with the nucleophilicity sequence of the diamines from the results of molecular modeling and ^{1}H NMR. We also noticed that HPMDA-based polyimides displayed lower number-average molecular weights than 6FDA-series with the same diamine. This might be attributed to the relatively weak electron withdrawing of the cycloaliphatic dianhydride.

The anticipated chemical structures of these poly(benzimidazole imide)s were evidenced by ATR-FTIR (Fig. 4). The characteristic bands at around 1785 cm^{-1} for imide C═O asymmetric stretching, 1706 cm^{-1} for imide C═O symmetric stretching and 1367 cm^{-1} for imide C—N stretching confirmed the formation of imide ring. The peak corresponding to the C═O in intermediate amic acid (1660 cm^{-1}, gray band domain) was hardly observed, which explained the high imidization degree of all polyimide films [40,41]. The presence of peaks at 1303 cm^{-1} (imidazole breathing) and absence of peaks at ~3405 cm^{-1} (imidazole NH stretching) was indicative of the successful incorporation of N-substituted imidazole ring [42].

The effect of different 2′-substituents on the geometric conformation of the polyimides was evaluated by molecular modeling using Materials Studio software. There was one repeat unit that may be significantly affected, as shown in Fig. 5, in which the energy variation of the model unit as the dihedral angle (α) was presented. As the result of the geometric optimization conformations, the α with the lowest energy conformation in 5b-PIs was larger than that in 5a-PIs. That is, 5b-PIs with 2′-CF_3 possessed more conformations significantly deviating from coplanarity compared to the 2′-CH_3-connecting 5a-PIs when they were derived from the same dianhydride. The result confirmed the role of 2′-CF_3 group in enhancing the amount of backbone noncoplanar segments with its steric hindrance, which was responsible for the loosen chain packing of the corresponding polyimides.

The molecular packing density in the PBII films was evaluated through their FFV, which was calculated from density measurements. The FFV values ranged from 0.143 to 0.189 based on molecule

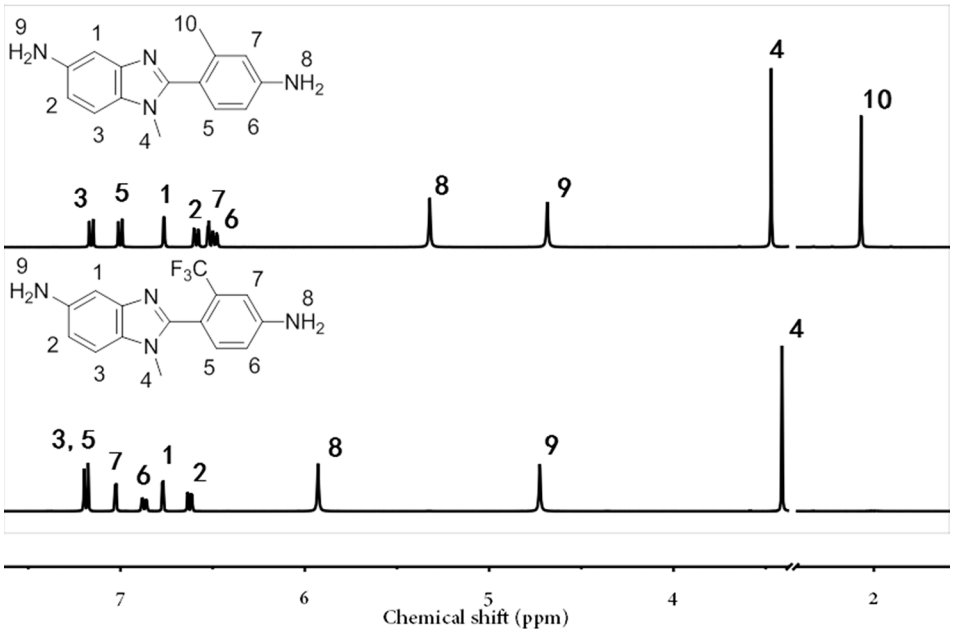

Fig. 2. ^{1}H NMR spectra (600 MHz, in DMSO-d_6) of the benzimidazole-containing diamines (5a and 5b).

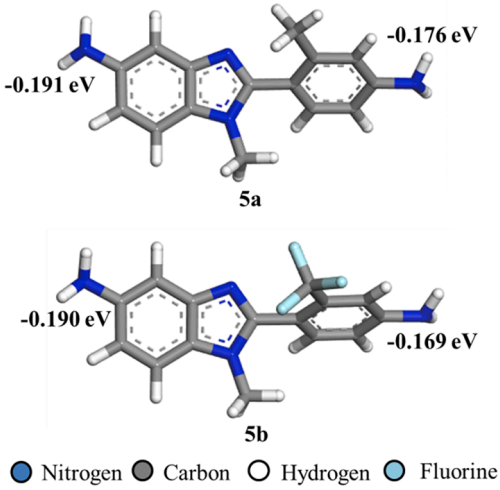

Fig. 3. The optimized geometries of the benzimidazole diamines and the net charges of their terminal amino groups, calculated using the Dmol3 program embedded in the Materials Studio.

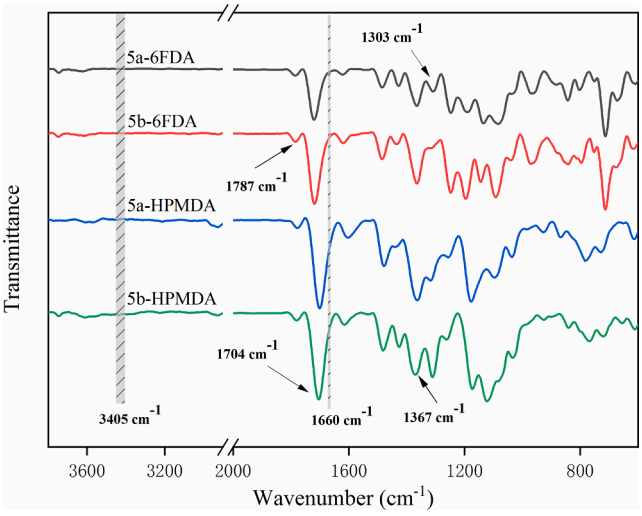

Fig. 4. ATR-FTIR spectra of the poly(benzimidazole imide) films.

Table 1
Molecular weights and packing parameters of the poly(benzimidazole imide)s.

PIs	M_n[a] ($\times 10^4$ g/mol)	M_w[a] ($\times 10^4$ g/mol)	PDI	ρ (g/cm^3)[b]	FFV[c]
5a-6FDA	5.70	9.06	1.59	1.4001	0.160
5b-6FDA	5.18	8.61	1.66	1.4136	0.189
5a-HPMDA	4.62	8.04	1.74	1.2962	0.143
5b-HPMDA	4.26	8.02	1.88	1.3189	0.187

[a] Relative to polystyrene standards.
[b] The buoyancy method with anhydrous ethanol.
[c] Calculated through film density.

configuration, as list in Table 1. As known, larger structural distortions lower chain packing coefficient, resulting in the increase in the polymer FFV [43,44]. The bent and twisted conformation in the obtained diamines could produce large FFV values for the corresponding PIs. The values of the PBIIs containing 5b were greater than those of the PBIIs derived from 5a. Because 5b had a higher level of non-coplanarity than 5a, introduction of the obviously twisted units from 5b into the PI backbones brought them with looser chain packing, which was confirmed by their molecular modeling. Additionally, 6FDA-based fully aromatic PBIIs showed higher FFV than the corresponding semi-aromatic ones. This indicated that the pair of bulky trifluoromethyl groups in the 6FDA played an important role in enhancing the free volume of the resulting films, which was the same with previous findings [18].

To further explain the free volume behavior of these PBII films, wide-angle X-ray diffraction (WAXD) results had been given, as shown in Fig. 6. All PBII films exhibited a broad diffraction halo at 2θ near 15°, suggesting their amorphous character. The phenomena were not in accordance with the traditional PBIIs which possessed dense chain packing and highly ordered molecular arrangements with their unique H-bondings [45,46]. Herein, the formation of such hydrogen bonds had

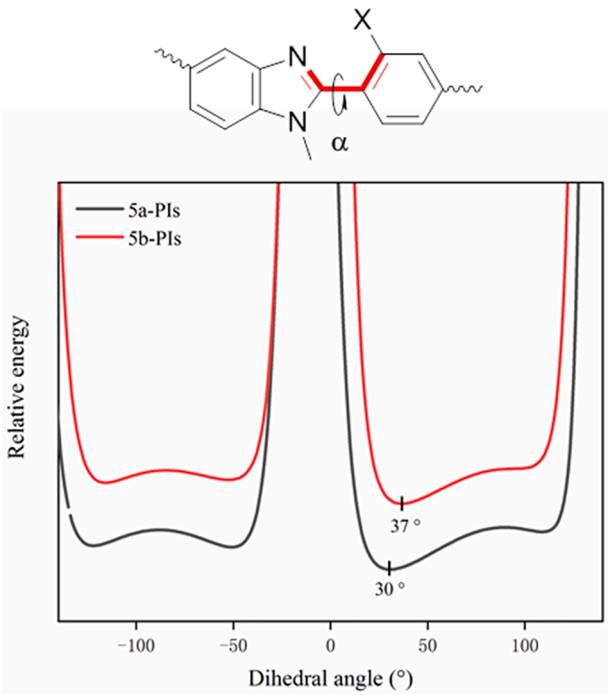

Fig. 5. Energy variation of one repeat unit for the poly(benzimidazole imide)s, determined by the conformers program in Materials Studio.

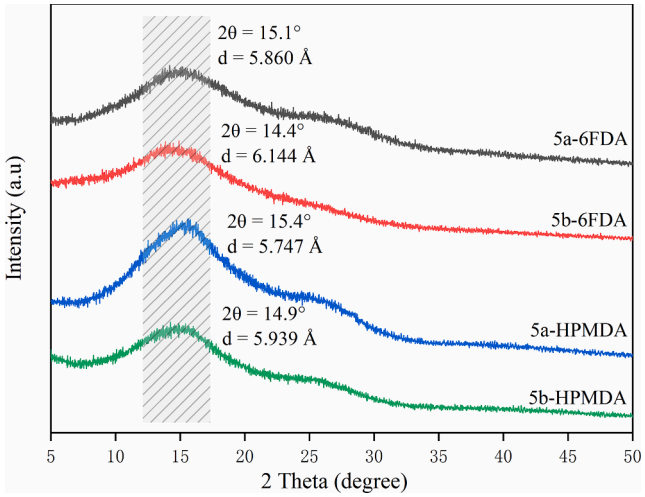

Fig. 6. WAXD curves of the poly(benzimidazole imide) films.

been completely forbidden by the N-substituents, and the asymmetric and noncoplanar structures from 5a and 5b enhanced the difficulty of the tight molecular aggregation formation for the polyimides containing them. In the result, peaks at $2\theta = \sim 15^{\circ}$ could be assigned to the average interchain packing in the polyimides and the calculated *d*-spacing values (5.747–6.144 Å) were close to the chain-chain distances [47,48]. The order was 5b-PIs > 5a-PIs for the given dianhydride and 6FDA-PIs > HPMDA-PIs for the same diamine, coinciding well with the their free volume values.

3.3. Solubility

It is well known that polyimides containing unsymmetrically structured rings possess improved solubility behavior, which facilitates processing in the materials formation [49]. Nonetheless, most of the reported PBIIs displayed poor solubility in the organic solvents with their dense molecular packing caused by the hydrogen bonds. Comparing with the above cases, a prominent solubility was obvious; all PBIIs were soluble in most polar organic solvents (Table 2). The significantly asymmetry/distorted steric structures resulted from the modified benzimidazole diamines were able to inhibit polyimide chain stacking, and consequently solvent molecule penetrated readily [50,51]. The effect was greater in the case of the 2′-CF_3 substituted N-methyl benzimidazole diamine than that of the 2′-CH_3 substituted ones, thus, 5b-derived PBIIs with the looser molecular packing displayed better solubility compared to 5a-based counterparts for the same dianhydride. Similarly, incorporation of lager structural distortions from 6FDA in the PBII chains resulted in lower packing degree compared to that of the PBII arisen from HPMDA; so the PBII derived from 5b and 6FDA displayed the best solubility in the given system.

3.4. Water absorption

The polymer H_2O-absorption character is susceptible to their chain packing as well as the content of polar units and hydrophilic groups. Benzimidazole moieties, as water-affinity-promoting structures, tend to form H-bonding with water molecules, and the benzimidazole-containing polymers generally display a high water absorption (W_A) value [52]. For example, PBIIs derived from PABZ had W_A up to 6%; and the value of poly(2,2′-m-(phenylene)-5,5′-bibenzimidazole) (PBI) was >15% [29,53,54]. In the series shown, the optimized PBIIs showed W_A values of 0.6 ~ 1.2% (Table 3), which was close to that of the conventional PI systems. The cause for the abnormal W_A values was that the N-CH_3 effectively blocked the formation of hydrogen-bonded water molecules as described in our previous research [29]. In contrast, the W_As were in the order: 5b-PIs < 5a-PIs and 6FDA-PIs < HPMDA-PIs, respectively. The trend was related to that the increased content of trifluoromethyl units with the lowest polarizability per unit volume could further reduce the water absorption values of the related polymers. Another factor influencing W_A was the content of highly polar imide units; and usually, the W_As increased as the polar content increased for polyimides. Hence, W_A values tended to decrease with an increase of the dianhydride molecular weight: the values of 6FDA-PIs were lower than that of HPMDA-PIs when they were prepared from the same diamines. In summary, the structure-optimized PBIIs were expected to solve a series of disadvantages (e.g., package cracking, degradation of dielectric properties and so on) resulted from high W_A for the traditional PBIIs.

3.5. Optical properties

As depicted in Table 4 and Fig. 7, the synthesized imidazole diamines were effective to erase traditional PBII film dark coloration for all systems. In particular, the semi-aromatic series completely eliminated PI yellow intensities (b* = 1.42–1.97, YI = 2.16–3.10 and T_{400} = 76–80%). This verified that the obtained diamines caused positive result on the film coloration; that is, the unique bent and twisted conformation was much effective for enhancing the difficulty of CTC formation through disturbing the conjugation and packing of polyimide chains. Moreover, an improvement of optical properties occurred for 5b-PBIIs versus 5a-PBIIs, highlighting the relatively weakened electron-donating effect of

Table 2
Solubility of the poly(benzimidazole imide) films.

PIs[a]	m-Cresol	NMP	DMAc	DMSO	DMF	THF	$CHCl_3$
5a-6FDA	+	+	+	±	±	±	±
5b-6FDA	+	+	+	+	+	+	±
5a-HPMDA	+	+	+	±	±	–	–
5b-HPMDA	+	+	+	+	+	±	–

+, soluble at room temperature; ±, partially soluble or swelling; –, insoluble.
[a] Solubility was determined with 10 mg of polyimide films in 1 mL of solvent at room temperature for 24 h.

Table 3
Basic properties of the poly(benzimidazole imide)s.

PIs	T_g[a] (°C)	$T_{d5\%}$[b] (°C)	CTE[c] (ppm/K)	E (GPa)	σ (MPa)	ε (%)	W_A (%)
5a-6FDA	371	505	48.9	3.3	135	8.7	0.9
5b-6FDA	360	498	52.2	3.2	114	7.6	0.6
5a-HPMDA	421	465	48.0	2.8	109	84.3	1.2
5b-HPMDA	409	446	50.2	2.8	100	71.6	1.1

[a] Glass transition temperature measured by DMA at a heating rate of 5 °C min^{-1} at 1 Hz.
[b] 5% weight loss temperature measured by TGA in nitrogen at a heating rate of 5 °C min^{-1}.
[c] Coefficient of thermal expansion along the X–Y direction, measured in the range of 150–250 °C at a heating rate of 5 °C min^{-1}.

Table 4
Optical properties of the poly(benzimidazole imide) films.

PIs[a]	d (μm)	L*	a*	b*	YI	λ_{cutoff} (nm)	T_{400} (%)
5a-6FDA	22	95.52	−4.53	12.05	16.52	379	14
5b-6FDA	21	95.82	−4.43	10.96	10.43	346	56
5a-HPMDA	21	95.99	−0.16	1.97	3.10	335	76
5b-HPMDA	23	96.05	−0.06	1.42	2.16	330	80

[a] d is film thickness. L* refers to lightness: 100 means white, while 0 indicates black. A positive a* means red color, a negative a* indicates green color. A positive b* means yellow color, a negative b* indicates blue color. YI means yellowness index. T_{400} means transmittance at 400 nm.

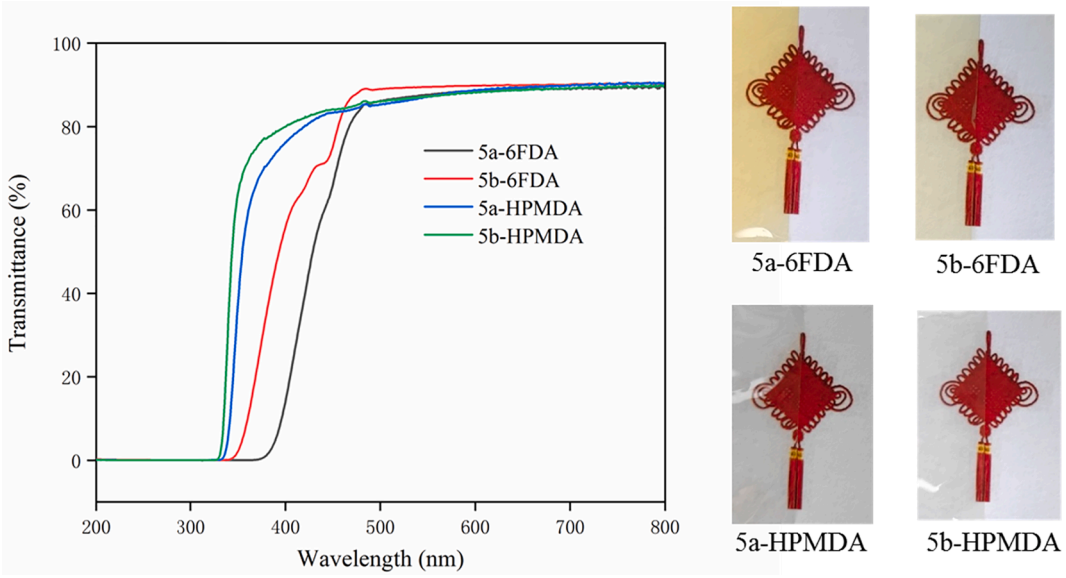

Fig. 7. UV–vis spectra and images of the poly(benzimidazole imide) films.

the 2′-CF_3 substituted diamine. This influence was greater in the full-aromatic series than that of the semi-aromatic series, due to the further optical improvement resulted from the fully alicyclic HPMDA. Indeed, compared with aromatic dianhydrides, alicyclic ones possessed inferior proton-accepting ability, leading to reduced CT interaction in the semi-aromatic polyimide films. Based on the combined effect, 5b-HPMDA exhibited the super optical data (b* = 1.42, YI = 2.16 and T_{400} = 80%) in this system.

3.6. Thermal properties

As known, when polyimides experience a high temperature, the rigid conjugated backbones facilitate the heat conduction along the chains, so polyimides with rigid chains usually possess higher thermal decomposition temperatures than those containing flexible bonds [55]. According to the theory, these rigid benzimidazole diamines were specifically effective for retaining polyimide superiority on the heat resistance. Thus, this series of poly(benzimidazole imide)s had relatively good thermal stability as suggested from the 5% weight loss values ($T_{d5\%}$ = 446–505 °C) under a nitrogen atmosphere, as shown in Fig. 8 and Table 3. Generally, the $T_{d5\%}$ values decreased to some degree when cycloaliphatic dianhydrides were used because of the low chemical heat resistance of alicyclic units [12,56]. However, the $T_{d5\%}$ of these HPMDA-PIs maintained relatively high values, e.g., 446 °C for 5b-HPMDA.

A T_g-transparency diagram was displayed in Fig. 9. Many engineering polymers showed excellent optical transparency, whereas their T_gs could not exceed 300 °C [9,10,57,58]. Conversely, polyimides tended to possess outstanding heat resistance (T_g > 300 °C) with losing transparency. Benzimidazole polyimide film (PABZ-BPDA), as a typical case, had a T_g exceeding 400 °C and none transmittance at 400 nm [33]. In fact, some modified PIs had partially achieved the colorless high-T_g targets (T_{400} > 80%, T_g > 300 °C) [56,59–61]. However, these were beyond the super candidates because of their T_gs less than 400 °C. Herein, the T_gs determined by the peak temperature of the tan delta curve ranged from 360 to 421 °C (Fig. S4) for the given PBIIs, which were higher than the values of PIs came from the same dianhydrides [59–61]. The intrinsic cause was that the typical asymmetric structures of benzimidazole diamines could be able to forbid the π-flip rotational

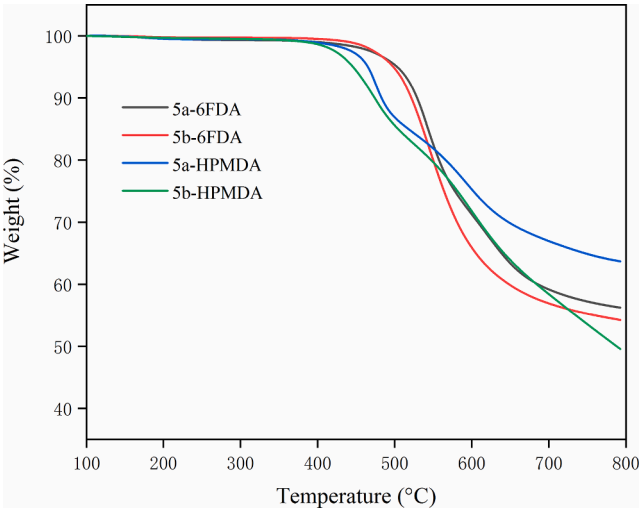

Fig. 8. TGA curves of the poly(benzimidazole imide) films under a nitrogen atmosphere.

motions with their significant steric hindrance when polyimides experienced a high temperature [24]. Regardless of steric hindrance effects, the strong intermolecular interaction also played an important role in leading to an increase in T_g values. Therefore, for certain dianhydrides, the T_g values of 5a-based PIs were about 10 °C higher than those of 5b-based series, which was attributed to the stronger interaction between the molecular chains caused by the more effective chain-segment packing in 5a-series. On the other hand, because the "dish" shapes of HPMDA facilitated the dense chain packing [56], the PBIIs derived from the alicyclic dianhydride had closer chain-chain distance and higher chain-chain interaction compared to 6FDA-ones. Thus, the semi-aromatic PBIIs exhibited the largest T_g values (≥400 °C), which was sufficient for the special high-temperature processing.

The dimensional stability of these PBII films was estimated by their CTE values and the results showed a common level ranging 48.0–52.2 ppm K^{-1} (Table 3, Fig. S5). The CTEs are usually susceptible to the degree of in-plane orientation that was governed by interchain interaction and chain stiffness/linearity for polyimides [48,62]. In this case, there existed regular differences in the given CTE results; compared with 5a, the employ of 5b suppressed the interaction between polymer chains because of its more twisted steric structures, thus, 5b-PBIIs displayed higher CTE values than 5a-PBIIs for a certain dianhydride. On the other hand, the nonlinear/non-coplanar structures of 6FDA were responsible for a CTE increase, wherefore the values of the full-aromatic polyimides were higher than those of the cases based on HPMDA.

3.7. Mechanical properties

Mechanical analysis data of these PBII films were summarized in Fig. S6 and Table 3. It gave tensile modulus from 2.8 to 3.3 GPa without significant difference. In contrast, obvious distinctions were observed in the film flexibility as suggested from their ε values; the semi-aromatic PBIIs showed prominent toughness, e.g., ε = 84.1% for 5a-HPMDA and 71.6% for 5b-HPMDA. This reflected the chain slippage in the plastic deformation region could be allowed when intermolecular forces were significantly weakened in the HPMDA-derived PBIIs, whereas the full-aromatic series with relatively rigid backbones displayed inferior elongation at break because of insufficient chain entanglement. Indeed, the full-aromatic PBIIs possessed a certain degree of superiority in tensile strength, and this was owing to their high molecular weights. Also,

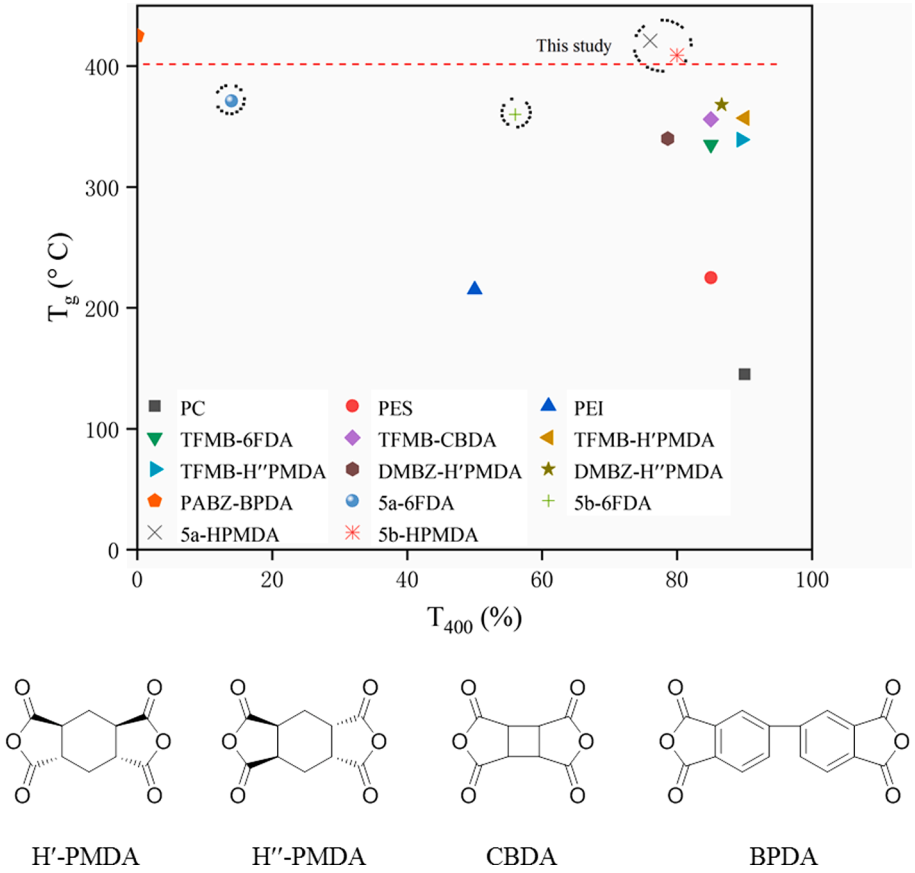

Fig. 9. Transparency-T_g diagram and some commercial dianhydride structures (PC: polycarbonate, PES: poly (ether sulfone), PEI: poly(ether imide)) [9,10,32,57–61].

the σ values of polymers were influenced not only by the molecular weight but also by the intermolecular interactions affected by the chemical structures. The more twisted conformations in 5b obviously reduced the polyimide intramolecular interaction, and that is 5b-PBIIs with looser chain packing would have relatively weaker tensile strength than 5a-ones. In summary, the excellent flexibility, high initial modulus (exceed 2.0 GPa) and good tensile strength (exceed 100 MPa) of these PBII films were sufficient for the optical application [30].

4. Conclusion

Two novel benzimidazole diamines (5a and 5b) with noncoplanar segments were synthesized for obtaining colorless polyimide films. The experimental results illustrated that these diamines could effectively disturb polymer chain stacking and rotational motion by their bent/twisted steric structure, which led to a balanced optimization in the optical transparency and thermal properties of polyimides. Among them, 5b-based PBIIs with 2′-CF_3 incorporating in the imidazole ring displayed remarkably desirable properties, for example, T_g = 409 °C, T_{400} = 80% and b* = 1.42 for 5b-HPMDA. In addition, the adjusting modified PBIIs possessed some prominent advantages compared to the traditional PBIIs: enhanced solution processability and drastically decreased W_A. These are expected to break through the bottleneck of poly(benzimidazole imide)s in the manufacturing and application, and expand their use in the field of superheat-resistant optical plastic films.

CRediT authorship contribution statement

Xiaoying Yan: Data curation, Writing – original draft. **Fengna Dai:** Software. **Zhao Ke:** Writing – review & editing. **Kuangguo Yan:** Supervision. **Chunhai Chen:** Resources. **Guangtao Qian:** Project administration. **Hui Li:** Funding acquisition.

Declaration of Competing Interest

The authors declare that they have no known competing financial interests or personal relationships that could have appeared to influence the work reported in this paper.

Acknowledgements

This work was supported by Science and Technology Planning Project of Guangdong Province (CN) (2020B010182002).

Appendix A. Supplementary material

Supplementary data to this article can be found online at https://doi.org/10.1016/j.eurpolymj.2021.110975.

References

[1] C. Yi, W. Li, S. Shi, K. He, P. Ma, M. Chen, C. Yang, High-temperature-resistant and colorless polyimide: Preparations, properties, and applications, Sol. Energy 195 (2020) 340–354.
[2] L. Fang, J. Sun, X. Chen, Y. Tao, Q. Fang, Phosphorus- and sulfur-containing high-refractive-index polymers with high T_g and transparency derived from a bio-based aldehyde, Macromolecules 53 (2020) 125–131.
[3] K. Hu, Q. Ye, Y. Fan, J. Nan, F. Chen, Y. Gao, Y. Shen, Preparation and characterization of organic soluble polyimides with low dielectric constant containing trifluoromethyl for optoelectronic application, Eur. Polym. J. 157 (2021) 110566.
[4] M.C. Choi, Y. Kim, C.S. Ha, Polymers for flexible displays: From material selection to device applications, Prog. Polym. Sci. 33 (2008) 581–630.
[5] Q. Wu, X. Ma, F. Zheng, X. Lu, Q. Lu, High performance transparent polyimides by controlling steric hindrance of methyl side groups, Eur. Polym. J. 120 (2019) 109235.
[6] S. Nakano, N. Saito, K. Miura, T. Sakano, T. Ueda, K. Sugi, A. Ishida, Highly reliable a-IGZO TFTs on a plastic substrate for flexible AMOLED displays, J. Soc. Inf. Disp. 20 (2012) 493–498.
[7] S.E. Burns, K. Reynolds, W. Reeves, M. Banach, T. Brown, K. Chalmers, M. D. McCreary, Flexible Active-Matrix Displays, SID Symp. Dig. Tech. Pap. 36 (2005) 19–21.
[8] G.H. Gelinck, H.E.A. Huitema, M. Van Mil, E. Van Veenendaal, P.J.G. Van Lieshout, F.J. Touwslager, Flexible QVGA active matrix displays based on organic electronics, SID Symp. Dig. Tech. Pap. 36 (2005) 6–9.
[9] M. Yan, T.W. Kim, A.G. Erlat, M. Pellow, D.F. Foust, J. Liu, A.R. Duggal, A transparent, high barrier, and high heat substrate for organic electronics, Proc. IEEE 93 (2005) 1468–1477.
[10] J. Jang, S.H. Han, High-Performance OTFTs on Flexible Substrate, SID Symp. Dig. Tech. Pap. 36 (2005) 10–13.
[11] T. Agag, T. Koga, T. Takeichi, Studies on thermal and mechanical properties of polyimide-clay nanocomposites, Polymer 42 (2001) 3399–3408.
[12] Y. Zhuang, J.G. Seong, Y.M. Lee, Polyimides containing aliphatic/alicyclic segments in the main chains, Prog. Polym. Sci. 92 (2019) 35–88.
[13] D.J. Liaw, K.L. Wang, Y.C. Huang, K.R. Lee, J.Y. Lai, C.S. Ha, Advanced polyimide materials: syntheses, physical properties and applications, Prog. Polym. Sci. 37 (2012) 907–974.
[14] C.E. Sroog, Polyimides, Prog. Polym. Sci. 16 (4) (1991) 561–694.
[15] J. Miao, X. Hu, X. Wang, X. Meng, Z. Wang, J. Yan, Colorless polyimides derived from adamantine-containing diamines, Polym. Chem. 11 (2020) 6009–6016.
[16] Z. Yang, H. Guo, C. Kang, L. Gao, Synthesis and characterization of amide-bridged colorless polyimide films with low CTE and high optical performance for flexible OLED displays, Polym. Chem. 12 (2021) 5364.
[17] X. Hu, H. Mu, Y. Wang, Z. Wang, J. Yan, Colorless polyimides derived from isomeric dicyclohexyl-tetracarboxylic dianhydrides for optoelectronic applications, Polymer 134 (2018) 8–19.
[18] Y. Zhuang, R. Orita, E. Fujiwara, Y. Zhang, S. Ando, Colorless partially alicyclic polyimides based on tröger's base exhibiting good solubility and dual fluorescence/phosphorescence emission, Macromolecules 52 (2019) 3813–3824.
[19] R.S. Mulliken, Molecular Compounds and their Spectra II, J. Am. Chem. Soc. 74 (1952) 811–824.
[20] M. Hasegawa, K. Horie, Photophysics, photochemistry, and optical properties of polyimides, Prog. Polym. Sci. 26 (2) (2001) 259–335.
[21] S. Ando, T. Matsuura, S. Sasaki, Coloration of aromatic polyimides and electronic properties of their source materials, Polym. J. 29 (1997) 69–76.
[22] C.P. Yang, Y.Y. Su, Colorless polyimides from 2,3,3′,4′-biphenyltetracarboxylic dianhydride (α-BPDA) and various aromatic bis (ether amine)s bearing pendent trifluoromethyl groups, Polymer 46 (2005) 5797–5807.
[23] B. Li, Z. Yan, T. Zhang, S. Jiang, K. Wang, D. Wang, Y. Liu, Synthesis and properties of novel colorless and thermostable polyimides containing cross-linkable bulky tetrafluorostyrol pendant group and organosoluble triphenylmethane backbone structure, J. Polym. Sci. 58 (2020) 2355–2365.
[24] T. Okada, R. Ishige, S. Ando, Effects of chain packing and structural isomerism on the anisotropic linear and volumetric thermal expansion behaviors of polyimide films, Polymer 146 (2018) 386–395.
[25] M. Hasegawa, N. Sensui, Y. Shindo, R. Yokota, Improvement of thermoplasticity for s-BPDA/PDA by copolymerization and blend with novel asymmetric BPDA-based polyimides, J. Polym. Sci. Part B: Pol. Phys. 37 (17) (1999) 2499–2511.
[26] Y. Jiao, G. Chen, H. Zhou, F. Zhang, X. Chen, Y. Li, X. Fang, Synthesis and properties of processable poly (benzimidazole-imide)s based on 2-(3-aminophenyl)-5-aminobenzimidazole, J. Polym. Res. 26 (2019) 1–12.
[27] K.C. Chuang, J.D. Kinder, D.L. Hull, D.B. McConville, W.J. Youngs, Rigid-Rod Polyimides Based on Noncoplanar 4,4′-Biphenyldiamines: A Review of Polymer Properties vs Configuration of Diamines, Macromolecules 30 (1997) 7183–7190.
[28] F. Li, S. Fang, J.J. Ge, P.S. Honigfort, J.C. Chen, F.W. Harris, S.Z. Cheng, Diamine architecture effects on glass transitions, relaxation processes and other material properties in organo-soluble aromatic polyimide films, Polymer 40 (1999) 4571–4583.
[29] G. Qian, H. Chen, G. Song, F. Dai, C. Chen, J. Yao, Superheat-resistant polyimides with ultra-low coefficients of thermal expansion, Polymer 196 (2020) 122482.
[30] M. Lian, X. Lu, Q. Lu, Synthesis of superheat-resistant polyimides with high T_g and low coefficient of thermal expansion by introduction of strong intermolecular interaction, Macromolecules 51 (2018) 10127–10135.
[31] Y. Zhuang, X. Liu, Y. Gu, Molecular packing and properties of poly (benzoxazole-benzimidazole-imide) copolymers, Polym. Chem. 3 (2012) 1517–1525.
[32] S. Wang, H. Zhou, G. Dang, C. Chen, Synthesis and Characterization of Thermally Stable, High-Modulus Polyimides Containing Benzimidazole Moieties, J. Polym. Sci., Part A: Polym. Chem. 47 (8) (2009) 2024–2031.
[33] G. Qian, F. Dai, H. Chen, M. Wang, M. Hu, C. Chen, Y. Yu, Incorporation of N-phenyl in poly (benzimidazole imide)s and improvement in H_2O-absorbtion and transparency, RSC Adv. 11 (2021) 3770–3776.
[34] X. Wang, F. Chen, Y. Gu, Influence of electronic effects from bridging groups on synthetic reaction and thermally activated polymerization of bisphenol-based benzoxazines, J. Polym. Sci., Part A: Polym. Chem. 49 (6) (2011) 1443–1452.
[35] Y. Zhuang, J.G. Seong, Y.S. Do, H.J. Jo, M.J. Lee, G. Wang, Y.M. Lee, Effect of isomerism on molecular packing and gas transport properties of poly (benzoxazole-co-imide) s, Macromolecules 47 (2014) 7947–7957.
[36] H. Sun, COMPASS: An ab Initio Force-Field Optimized for Condensed-Phase Applications-Overview with Details on Alkane and Benzene Compounds, J. Phys. Chem. B. 102 (1998) 7338–7364.
[37] X. Ma, O. Salinas, E. Litwiller, I. Pinnau, Novel spirobifluorene-and dibromospirobifluorene-based polyimides of intrinsic microporosity for gas separation applications, Macromolecules 46 (2013) 9618–9624.
[38] A.A. Bondi, Physical Properties of Molecular Crystals Liquids, and Glasses, John Wiley & Sons, Inc., New York, 1968.

[39] A. Bondi, Van Der Waals Volumes and Radii, J. Phys. Chem. 68 (1964) 441–451.
[40] Y.K. Xu, M.S. Zhan, K. Wang, Structure and properties of polyimide films during a far-infrared-induced imidization process, J. Polym. Sci. B Polym. Phys. 42 (2004) 2490–2501.
[41] S. Diaham, M.L. Locatelli, T. Lebey, D. Malec, Thermal imidization optimization of polyimide thin films using Fourier transform infrared spectroscopy and electrical measurements, Thin Solid Films 519 (2011) 1851–1856.
[42] P. Musto, F.E. Karasz, W.J. MacKnight, Fourier transform infra-red spectroscopy on the thermo-oxidative degradation of polybenzimidazole and of a polybenzimidazole/polyetherimide blend, Polymer 34 (1993) 2934–2945.
[43] C.Y. Park, E.H. Kim, J.H. Kim, Y.M. Lee, J.H. Kim, Novel semi-alicyclic polyimide membranes: synthesis, characterization, and gas separation properties, Polymer 151 (2018) 325–333.
[44] S.H. Kang, T. Aoki, G. Kwak, Molecular-spring shape-memory polymer based on energy elasticity and local phase transition, Macromolecules 52 (2019) 7984–7993.
[45] L. Luo, Y. Dai, Y. Yuan, X. Wang, X. Liu, Control of Head/Tail Isomeric Structure in Polyimide and Isomerism-Derived Difference in Molecular Packing and Properties, Macromolecul. Rapid. Comm. 38 (2017) 1700404.
[46] G. Song, X. Zhang, D. Wang, X. Zhao, H. Zhou, C. Chen, G. Dang, Negative in-plane CTE of benzimidazole-based polyimide film and its thermal expansion behavior, Polymer 55 (2014) 3242–3246.
[47] J. Wakita, S. Jin, T.J. Shin, M. Ree, S. Ando, Analysis of Molecular Aggregation Structures of Fully Aromatic and Semialiphatic Polyimide Films with Synchrotron Grazing Incidence Wide-Angle XRay Scattering, Macromolecules 43 (2010) 1930–1941.
[48] J.H. Jou, P.T. Huang, Effect of Thermal Curing on the Structures and Properties of Aromatic Polyimide Films, Macromolecules 24 (1991) 3796–3803.
[49] H. Choi, I.S. Chung, K. Hong, C.E. Park, S.Y. Kim, Soluble polyimides from unsymmetrical diamine containing benzimidazole ring and trifluoromethyl pendent group, Polymer 49 (2008) 2644–2649.
[50] D. Patterson, Free volume and polymer solubility. A qualitative view, Macromolecules 2 (1969) 672–677.
[51] P.A. Small, Some factors affecting the solubility of polymers, J. Appl. Chem. 3 (1953) 71–80.
[52] D.W. Tomlin, A.V. Fratini, M. Hunsaker, W.W. Adams, The role of hydrogen bonding in rigid-rod polymers: the crystal structure of a polybenzobisimidazole model compound, Polymer 41 (2000) 9003–9010.
[53] T.S. Chung, A critical review of polybenzimidazoles: historical development and future R&D, J. Macromol. Sci., Part C Pol. Rev. 37 (1997) 277–301.
[54] G. Qian, H. Chen, G. Song, J. Yao, M. Hu, C. Chen, Synthesis of polyimides with lower H_2O-absorption and higher thermal properties by incorporation of intramolecular H-bonding, J. Polym. Sci., Part A: Polym. Chem. 58 (2020) 969–976.
[55] Y.N. Sazanov, F.S. Florinsky, M.M. Koton, Investigation of thermal and thermooxidative degradation of some polyimides containing oxyphenylene groups in the main chain, Eur. Polym. J. 15 (1979) 781–786.
[56] M. Hasegawa, M. Fujii, J. Ishii, S. Yamaguchi, E. Takezawa, T. Kagayama, A. Ishikawa, Colorless polyimides derived from 1S,2S,4R,5R-cyclohexanetetracarboxylic dianhydride, self-orientation behavior during solution casting, and their optoelectronic applications, Polymer 55 (2014) 4693–4708.
[57] V.L. Calil, C. Legnani, G.F. Moreira, C. Vilani, K.D.C. Teixeira, W.G. Quirino, M. Cremona, Transparent thermally stable poly (etherimide) film as flexible substrate for OLEDs, Thin Solid Films 518 (2009) 1419–1423.
[58] R.O. Johnson, H.S. Burlhis, Polyetherimide: A new high-performance thermoplastic resin, J. Polym. Sci. Polym. Sym. 70 (1) (1983) 129–143.
[59] M. Hasegawa, D. Hirano, M. Fujii, M. Haga, E. Takezawa, S. Yamaguchi, A. Ishikawa, T. Kagayama, Solution-processable colorless polyimides derived from hydrogenated pyromellitic dianhydride with controlled steric structure, J. Polym. Sci. Part A Polym. Chem. 51 (3) (2013) 575–592.
[60] T. Matsuura, Y. Hasuda, S. Nishi, N. Yamada, Polyimide derived from 2,2′-bis (trifluoromethyl)-4,4'-diaminobiphenyl. 1. Synthesis andcharacterization of polyimides prepared with 2,2′-bis(3,4-dicarboxyphenyl)hexafluoropropane dianhydride orpyromellitic dianhydride, Macromolecules 24 (1991) 5001–5005.
[61] M. Hasegawa, Y. Watanabe, S. Tsukuda, J. Ishii, Solution-processable colorlesspolyimides with ultralow coefficients of thermal expansion foroptoelectronic applications, Polym. Int. 65 (2016) 1063–1073.
[62] M. Hasegawa, K. Okuda, M. Horimoto, Y. Shindo, R. Yokota, M. Kochi, Spontaneous molecular orientation of polyimides induced by thermal imidization. 3. Component chain orientation in binary polyimide blends, Macromolecules 30 (1997) 5745–5752.